

Striking Effects of Hydrodynamic Interactions on the Simulated Diffusion and Folding of Proteins

Tamara Frembgen-Kesner and Adrian H. Elcock*

Department of Biochemistry, University of Iowa, Iowa City, Iowa 52242

Received November 17, 2008

Abstract: Successful modeling of the processes of protein folding and aggregation may ultimately require accurate descriptions of proteins' diffusive characteristics, which are expected to be influenced by hydrodynamic effects; a comprehensive study of the diffusion and folding of 11 model proteins with an established simulation model extended to include hydrodynamic interactions between residues has therefore been carried out. Molecular simulations that neglect hydrodynamic interactions are incapable of simultaneously reproducing the expected experimental translational and rotational diffusion coefficients of folded proteins, drastically underestimating both when reasonable hydrodynamic radii are employed. In contrast, simulations that include hydrodynamic interactions produce diffusion coefficients that match very well with the expected experimental values for translation and rotation and also correctly capture the significant decrease in translational diffusion coefficient that accompanies protein unfolding. These effects are reflected in folding simulations of the same proteins: the inclusion of hydrodynamic interactions accelerates folding by 2–3-fold with the rate enhancement for the association of secondary structure elements exhibiting a strong sensitivity on the sequence-distance between the associating elements.

Introduction

Efforts to develop an understanding of the mechanistic details of protein folding have been pursued for many years (for reviews, see refs 1–3) and have taken on added significance recently with the realization that a number of pathologies (the so-called ‘conformational diseases’⁴) are caused by, or at least heavily associated with, protein misfolding and aggregation.⁵ Theoretical and computational studies have provided a number of insights into the folding of single, isolated proteins (e.g., refs 6–8), protein–protein association (e.g., refs 9–12), oligomerization (e.g., refs 13 and 14), domain-swapping (e.g., refs 15 and 16), and aggregation processes (e.g., refs 17–20).

Up to now, very few studies have focused on how well the extant simulation models capture the diffusive motions of protein chains, either with explicit solvent²¹ or implicit solvent methods.²² This, however, is an issue that warrants special attention for the modeling of aggregation or coupled

folding-association processes since both involve an interplay (or competition) between intramolecular folding and intermolecular association events, with the latter, in particular, having a clear potential for diffusion dependence. An indication that it might be important to pay particular attention to proteins' diffusive properties is given by the fact that a number of protein aggregation processes have already been described as being controlled by kinetic rather than strictly thermodynamic factors (e.g., refs 23 and 24). Full consideration of the issue requires asking whether simulation methods are capable of accurately capturing both the translational and rotational diffusive motions of protein chains and the changes in diffusive properties that accompany their folding and/or association.

Molecular simulations of protein folding and/or association events can be roughly divided into two categories depending on whether they use explicit or implicit models for the solvent. Explicit solvent simulations have the obvious advantage of being physically more complete in the sense that individual water molecules are allowed to play specific roles during folding or association. They have the very

* Corresponding author phone: (319)335-7894; fax: (319)335-9570; e-mail: adrian-elcock@uiowa.edu.

significant disadvantage however of being computationally demanding in comparison with corresponding implicit solvent simulations, and this expense has limited their use in the present context to a few heroic efforts in which either distributed computing resources (e.g., refs 13, 25, and 26) or highly parallelized architectures (e.g., refs 27–29) have been employed. Currently therefore, it is more common for protein folding simulations to employ implicit solvent models (e.g., refs 30 and 31). Of course, such models must attempt to incorporate in some way the energetic and dynamic influences that water exerts over the solute. The energetic effects of hydration—which are *not* the focus of the present work—can be implicitly modeled using continuum dielectric methods to account for electrostatic factors^{32,33} and solvent-accessible surface area-based approaches to describe hydrophobic contributions.^{34–36} Alternatively, for applications directed at studying protein folding and association processes, the issue of properly modeling the energetics is often sidestepped completely by using a native-centric ‘Gō’ model,³⁷ in which simple attractive potentials are applied to atom- or residue-pairs that form contacts in the native state, and purely repulsive potentials are applied to all other pairs. Despite the apparently drastic simplification involved in Gō-type models, the energy landscapes for folding obtained with them appear to capture a number of key features of experimental folding behavior.^{8,38–42}

The purely dynamic effects that would be exerted by the missing water molecules in implicit solvent simulations can be accounted for by the use of Langevin dynamics (LD) (discussed in refs 43 and 44) or Brownian dynamics (BD) algorithms,⁴⁵ and it is with the second of these methods that the present study is concerned. In both LD and BD, water implicitly appears in the equations of motion—in the form of its viscosity—in the diffusion tensor, **D** (see Methods); in BD implementations, **D**, a $3N \times 3N$ matrix (where N is the number of particles) determines both (a) the extent of coupling between force-induced displacements of solute particles and (b) the statistical properties of the random displacements that are applied to the solute particles.⁴⁵ Importantly, the diffusion tensor provides the means of including the effects of hydrodynamic interactions (HI) between solute particles (e.g., protein residues) into the equations of motion. There are several ways of conceptualizing HI; the simplest perhaps is to consider them as accounting for the fact that the displacement of one solute particle can have a ‘knock-on’ effect on a second nearby solute particle due to the displacement of intervening solvent molecules. Inclusion of HI therefore introduces correlations into the random, Brownian displacements experienced by neighboring solutes, such that they tend to be displaced in similar directions; neglect of HI (also known as the ‘free draining’ approximation⁴⁴) means that the Brownian displacements applied to neighboring solute particles are completely uncorrelated.

Given the above it is not hard to imagine that the inclusion of HI into simulations of polymers such as proteins might have a significant effect on their diffusive properties. In fact, there is a considerable body of literature in the polymer physics field that has already examined the effects of HI on

the translational diffusion of high molecular weight polymers. It was shown many years ago, for example,⁴⁶ that the inclusion of HI—modeled via the Kirkwood-Riseman approximation⁴⁷—successfully explains the $Mw^{-1/2}$ dependence observed for polymer translational diffusion coefficients in so-called θ conditions, whereas when HI are neglected, a much shallower, incorrect, Mw^{-1} dependence is obtained.^{48,49} More recently it has been shown that the inclusion of HI significantly increases the collapse rate of polymers in so-called ‘bad’ solvent conditions.^{50–54} While it is to be anticipated that these previous studies of simple polymers will provide useful clues to what might happen in proteins, very little attention has thus far been focused on the effects of HI on the folding and diffusion of actual protein chains.^{22,53} In fact, it has been recently reported that in regard to *unfolding*, simple homopolymers and protein chains appear to exhibit distinct behaviors.⁵⁵ We therefore have conducted a relatively systematic comparison of the effects of HI on the BD-simulated diffusion and folding of eleven proteins using an established simulation model; the results indicate that inclusion of HI is likely to be essential for correctly capturing the full range of diffusive behavior exhibited by folding protein chains.

Methods

The Proteins Studied. Eleven well-characterized proteins were chosen in order to cover a range of structural classes, subject to the restriction that they be sufficiently small (<150 residues) that complete sampling of their behavior would be computationally tractable. The proteins selected were as follows: the B1 immunoglobulin-binding domain of protein G (hereafter termed simply ‘protein G’),⁵⁶ B1 immunoglobulin-binding domain of protein L (protein L),⁵⁷ chymotrypsin inhibitor 2 (CI2),⁵⁸ barnase,⁵⁹ the fyn SH3 domain (fyn-SH3),⁶⁰ cold shock protein B (CSPB),⁶¹ intestinal fatty acid binding protein (IFABP),⁶² Semliki Forest viral capsid protein (SFVP),⁶³ λ -repressor,⁶⁴ colicin E9 immunity protein (Im9),⁶⁵ and apo-calmodulin (apoCaM).⁶⁶ The Protein Data Bank (PDB)⁶⁷ (<http://www.rcsb.org>) files used in these simulations, with the exceptions of SFVP and apoCaM, are identical with those listed in ref 68. The key characteristics of the proteins are summarized in Table 1. In addition to these complete proteins, an α -helix and a β -hairpin, both 16 residues in length, were also simulated; the structure of the former was taken from the first helix of λ -repressor, the latter from strands 6 and 7 of IFABP.

The Protein Model. The structural and energetic model used for the proteins in all simulations is a Gō-like model,³⁷ implemented in essentially the same manner as described by Clementi, Onuchic, and others.^{8,39,40,42} The all-atom structures of the proteins were reduced to simpler ‘bead-spring’ models and simulated at two different levels of detail. The first of these, which we refer to in the text by the shorthand expression ‘C α ’, represents each amino acid residue with a single bead, or pseudoatom, placed at the position of the C α atom. The second, finer level of detail, which we refer to by the abbreviation ‘SC’ (for Side Chain) represents residues again with a C α pseudoatom but supplemented by additional (up to three) pseudoatoms to model

Table 1. Details of the Proteins Studied

protein	PDB	fold type	number of domain(s)	number of C α atoms	number of SC atoms
α -helix		α -helix		16	
β -hairpin		β -sheet		16	
protein G	1PGA	mixed	one	56	141
protein L ^a	1HZ6	mixed	one	64	160
CI2	2CI2	mixed	one	65	165
barnase ^b	1BNI	mixed	two	108	269
fyn-SH3	1SHF	β -sheet	one	59	151
CSPB	1CSP	β -sheet	one	67	165
IFABP	1IFC	β -sheet	one	131	335
SFVP	1VCP	β -sheet	two	149	358
λ -repressor ^c	1LMB	α -helix	one	80	202
Im9 ^d	1IMQ	α -helix	one	86	216
apo-CaM ^d	1CFD	α -helix	two	148	380

^a Y47W mutant. ^b Added missing side chain atoms to Lys19, Glu60, Lys62, and Gln104 using WHATIF.⁶⁹ ^c Residues 6–85. ^d Averaged NMR structure.

the side chains. Full details of the latter model, which is conceptually similar to others previously presented in the literature,^{70,71} are given in the Supporting Information. The total numbers of pseudoatoms that were used to represent each protein are listed in columns five and six of Table 1 for the C α and SC descriptions, respectively.

Following the G \ddot{o} model approach, the interactions between all nonbonded pairs of pseudoatoms were assigned one of two energy functions. Pseudoatom pairs that formed a close contact in a protein's native state structure were assigned a favorable Lennard-Jones-type energy function in order to provide them with an energetic reward for forming such a contact during the simulations; pairs were considered to form a native contact if any of their constituent non-hydrogen atoms were within 5.5 Å of each other in the native state structure.³⁹ Following others,^{8,39,40,42} the form of this energy function was chosen to be

$$E_{ij}^{\text{native}} = \varepsilon [5(\sigma_{ij}/r_{ij})^{12} - 6(\sigma_{ij}/r_{ij})^{10}] \quad (1)$$

where ε is the energy well depth of the Lennard-Jones potential, r_{ij} is the distance between pseudoatoms i and j in the simulations, and σ_{ij} is the distance between the two pseudoatoms in the native state structure. For simulations of proteins in their folded states and for simulations of folding events, ε values of 0.60 and 0.25 kcal/mol were used for the C α and SC models, respectively; the former value was obtained from our previous work matching the experimental folding free energy of CI2 at 25 °C,⁴² the latter value was obtained here by performing similar 100 μ s-length simulations—and using histogram techniques^{72,73}—to reproduce the folding free energy of protein L.⁷⁴ For simulations of proteins in unfolded states, a much smaller ε value of 0.05 kcal/mol was used for both C α and SC models. Pseudoatom pairs separated by four or more bonds that do not form a close contact in the native state structure were assigned a purely repulsive potential

$$E_{ij}^{\text{non-native}} = \varepsilon (\sigma/r_{ij})^{12} \quad (2)$$

with σ in this case being a constant value (4 Å) and ε being assigned the value of 0.60 kcal/mol.

For bonding interactions between the pseudoatoms, standard molecular mechanics terms were used,⁴³ with the total bonded energy of the protein being written

$$E_{\text{bonded}} = \sum_{\text{bonds}} K_r(r-r_0)^2 + \sum_{\text{angles}} K_\theta(\theta-\theta_0)^2 + \sum_{\text{dihedrals}} K_\varphi^{(n)}[1-\cos(n(\varphi-\varphi_n))] \quad (3)$$

where r , θ , and φ are (pseudo)bond lengths, angles and dihedrals, respectively, and r_0 and θ_0 are the corresponding native state bond lengths and angles; φ_1 and φ_3 are phase angles which define the energy maxima of the dihedral angles. Following others,^{8,39,40,42} the bond and angle force constants K_r and K_θ were set to 100 kcal/mol/Å and 20 kcal/mol/rad, respectively. For folding simulations, the force constants for the two dihedral rotations $K_\varphi^{(1)}$ and $K_\varphi^{(3)}$ were set to 0.50 and 0.25 kcal/mol, respectively (for C α models), and to 0.41 and 0.21 kcal/mol, respectively (for SC models). These values were chosen in order to maintain an appropriate balance between the nonlocal and local driving forces for folding, since this balance has been shown to affect the cooperativity of folding equilibria simulated with G \ddot{o} models.^{8,42,75} For unfolded state simulations with both models, $K_\varphi^{(1)}$ and $K_\varphi^{(3)}$ were set to weaker values of 0.10 and 0.05 kcal/mol, respectively.

The Simulation Algorithm. The time-dependent conformational behavior of the proteins was simulated using the Brownian dynamics (BD) algorithm of Ermak and McCammon⁴⁵

$$\mathbf{r}_i(t + \Delta t) = \mathbf{r}_i(t) + \sum_j \mathbf{D}_{ij} \mathbf{F}_j \Delta t / k_B T + \mathbf{R}_i \quad (4)$$

where $\mathbf{r}_i(t)$ is the position vector of the i th pseudoatom at time t ; Δt is the simulation time step, \mathbf{D}_{ij} is the i,j th 3×3 submatrix of the diffusion tensor \mathbf{D} (a $3N \times 3N$ matrix, where N is the number of pseudoatoms in the simulated system); \mathbf{F}_j is the total force acting on the j th pseudoatom; and \mathbf{R}_i is a random displacement applied to the i th pseudoatom (see below); k_B is Boltzmann's constant, and T is the temperature in Kelvin.

The diffusion tensor is perhaps best thought of as a $N \times N$ supermatrix of 3×3 matrices, with each individual 3×3 submatrix describing the coupling between the x , y , and z components of motion for a pair of pseudoatoms i and j . For simulations that do not include hydrodynamic interactions (also known in the literature as the 'free draining' approximation⁴⁴), the only nonzero elements in the entire diffusion tensor are to be found along the diagonals of the 3×3 submatrices for those cases where pseudoatom $i = j$; as is usual,⁴⁵ these diagonal elements were calculated from the Stokes–Einstein relation $\mathbf{D}_{ii} = k_B T / 6\pi\eta_s a$ where η_s is the viscosity of the solvent (for water, $\eta_s = 0.89$ cP at 25 °C), and a is the hydrodynamic radius of the pseudoatom. For all simulations, the hydrodynamic radii assigned to pseudoatoms were 5.3 Å and 3.5 Å for the C α and SC models, respectively (see the next section for the derivation of these values). For simulations that include hydrodynamic interactions, the elements of the 3×3 matrices for interactions between pseudoatoms i and j ($i \neq j$) are nonzero, which has the result that the displacement of a pseudoatom i is directly affected by the forces acting on a pseudoatom j to which it is hydrodynamically coupled (see eq 4). In the present work the elements of the \mathbf{D}_{ij} submatrices were computed using

equations due to Rotne and Prager⁷⁶ and Yamakawa.⁷⁷ The complete set of equations used to compute \mathbf{D} is therefore

$$\mathbf{D}_{ii} = (k_B T / 6\pi\eta_s a) \mathbf{I} \quad (5a)$$

$$\mathbf{D}_{ij} = (k_B T / 8\pi\eta_s) \{ (1/r_{ij}) [(1 + 2a^2/3r_{ij}^2) \mathbf{I} + (1 - 2a^2/r_{ij}^2)(\mathbf{r}_{ij}\mathbf{r}_{ij}/r_{ij}^2)] \} \text{ for } r_{ij} \geq 2a \quad (5b)$$

$$\mathbf{D}_{ij} = (k_B T / 8\pi\eta_s) \{ (1/r_{ij}) [(r_{ij}/2a)(8/3 - 3r_{ij}/4a) \mathbf{I} + (r_{ij}/4a)(\mathbf{r}_{ij}\mathbf{r}_{ij}/r_{ij}^2)] \} \text{ for } r_{ij} < 2a \quad (5c)$$

where \mathbf{I} is a unit 3×3 matrix (1 for all diagonal elements; 0 for all nondiagonal elements), r_{ij} is the distance between pseudoatoms i and j , and \mathbf{r}_{ij} is the vector connecting them.

The fluctuation–dissipation theorem ensures that correct Boltzmann sampling is obtained by specifying a relationship between the diffusion tensor and the statistical properties required of the random displacements applied to the pseudoatoms. Formally these requirements can be written as

$$\langle \mathbf{R}_i \cdot \mathbf{R}_j \rangle = 6\mathbf{D}_{ij}\Delta t \text{ and } \langle \mathbf{R}_i \rangle = 0 \quad (6)$$

When hydrodynamic interactions are modeled, the $3N$ vector of correlated random displacements is obtained by multiplying a $3N$ vector of uncorrelated random numbers (with zero mean and unit variance) by the ‘square root’ matrix \mathbf{S} , which is generated from a factorization of the matrix \mathbf{D} , such that^{45,78}

$$\mathbf{D} = \sum_i \mathbf{S}_{ii} \mathbf{S}_{ji} \quad (7)$$

Thus the coupling of motion of pseudoatoms i and j specified in the diffusion tensor appears also in the random displacements. In the present study, factorization of the matrix \mathbf{D} was achieved by performing a (computationally expensive) Cholesky decomposition.^{78–80}

Software for conducting all BD simulations was written in-house;⁴² FORTRAN code implementing the Rotne–Prager–Yamakawa diffusion tensor calculation and the Cholesky decomposition was obtained from routines written by Allen and Tildesley.⁴³

Simulation Details. For all eleven proteins studied, separate BD simulations were performed to investigate the effects of hydrodynamic interactions (HI) on the simulated diffusional properties of the proteins in their folded and unfolded states using both C α and SC models. Additional studies were performed to investigate the effects of hydrodynamic interactions on folding pathways and rates using C α models of all eleven proteins and SC models of three representative proteins, protein L, CSPB, and λ -repressor. In all simulations that started from the unfolded state, initial conformations were generated by randomly assigning dihedral angles such that no steric clashes were introduced.

For simulations aimed at measuring diffusive characteristics, we found that the computed translational and rotational diffusion coefficients obtained from the BD simulations were essentially insensitive to the choice of time step (see the Supporting Information); because of this, timesteps of 40 and 20 fs were used for HI and non-HI simulations, respectively. For simulations aimed at investigating the actual folding behavior of proteins more care was found to be

needed in the choice of simulation timesteps, especially in the case of simulations performed with the more detailed SC model, since simulations that included HI typically produced slightly lower energies (i.e., more stable trajectories) for a given time step than did non-HI simulations. The origins of this effect almost certainly lie in the fact that HI promote correlated motions for closely separated pseudoatoms and therefore tend to suppress abrupt changes in bonding and short-range steric interactions that would otherwise occur in corresponding non-HI simulations. This becomes an issue because the simulated folding rates of proteins are often strongly dependent on their thermodynamic stability, so artifactual differences between a protein’s stability in the presence and absence of HI due to a poor choice of timesteps could cause misleading differences in their observed rates of folding. (It is worth noting that a similar dependence of experimental folding rates on thermodynamic stability is also observed.^{74,81,82}) To circumvent this issue, exploratory native-state simulations were performed for all eleven proteins using a range of timesteps, and a combination of timesteps that resulted in equivalent internal energies with and without HI were then selected; the timesteps chosen for HI and non-HI simulations ranged from 20 to 100 and from 10 to 100 fs, respectively. Full details of this procedure, showing the time step dependence of the proteins’ simulated energies, are provided in the Supporting Information.

In addition to finding that simulations with and without HI differed significantly in terms of their robustness to changing the timestep, we also found that they responded very differently to the inclusion of bond constraints. In order to allow longer timesteps in molecular dynamics (MD) and BD simulations it is common to constrain bonds to their equilibrium distances via application of an iterative constraint algorithm such as SHAKE⁸³ or LINCS.⁸⁴ In the present study, we used LINCS to constrain all pseudobonds in the non-HI simulations: in our hands this typically allowed us to increase the time step by a factor of 4. When included in HI simulations however, LINCS caused severe problems: in particular, it caused significant—and systematic—differences in the pseudobond angle energies that could not be resolved by choosing a different time step. To our knowledge this effect has not been directly reported in the literature, although the use of HI with the SHAKE constraint algorithm has been previously reported to affect transport coefficients⁸⁵ and the thermodynamics of β -hairpin folding.²² Conceptually, the effect almost certainly originates from the juxtaposition of an algorithmic ‘step’ that promotes correlated displacements of bonded atoms (the inclusion of HI) with one that promotes anticorrelated displacements (the imposition of bond constraints: adjusting the positions of atoms to reach an equilibrium separation distance must either involve them being moved toward or away from each other, both of which are anticorrelated motions). Because of this problem, all simulations that included HI were performed *without* bond constraints; instead, pseudobond lengths were continually monitored during the simulations, and, if deviating by more than 0.4 Å from their equilibrium values, the simulation was backtracked by ~ 10 ps and restarted (see the Supporting

Information for details). Results from control simulations that folded model proteins without HI and without using LINCS were compared to those from the two models used here (with HI, without bond constraints, and without HI, but with bond constraints). The difference in the treatment of pseudobonds between the two models had no significant effect on the folding results reported here.

In all simulations, a conventional neighbor list⁴³ was used to facilitate rapid calculation of nonbonded interactions between pseudoatoms; this list was recalculated every 200 fs. Pseudoatom pairs that did not form a contact in the native state structure were added to this list if their separation distance was 8 Å or less; pairs that did form a native contact were added to the list if their separation distance was within 9 Å of their distance in the native state structure. For simulations in which HI were included, the elements of the diffusion tensor and its Cholesky decomposition were recalculated every 1 ps; exploratory simulations indicated that updating the diffusion tensor at every time step made essentially no difference to the simulation observables (see the Supporting Information).

Determination of ‘Experimental’ Diffusion Coefficients.

Since experimental estimates of protein translational and rotational diffusion coefficients can vary significantly between groups and (especially) depending on the experimental technique employed,^{86,87} we chose to estimate the diffusional properties for the eleven proteins using a single method, the hydrodynamics program HYDROPRO,^{88,89} in previous studies the diffusion coefficients calculated with this method have been shown to be within 2 and 6% of the experimental values for translation and rotation, respectively. All ‘experimental’ diffusion coefficients referred to in this study are therefore *computed* values obtained by applying HYDROPRO to the all-atom PDB files of the eleven proteins (Table 1); in all of these calculations the recommended default hydrodynamic radius of 3.2 Å was applied to all atoms.⁸⁹ In addition to being used to compute ‘gold-standard’ ‘experimental’ diffusion coefficients for native state structures, HYDROPRO was also used to compute diffusion coefficients for unfolded state structures of each protein. These estimates were obtained by randomly selecting 5 snapshots each from HI and non-HI simulations of the unfolded C α model and submitting the 10 selected snapshots to HYDROPRO with a hydrodynamic radius of 5.3 Å assigned to each pseudoatom (see below for the derivation of this value).

For actual BD simulations of the folding and diffusion of the proteins, the pseudoatoms’ hydrodynamic radii used in eqs 5a–5c were determined in the following way. The C α structural models of all eleven proteins were each submitted to HYDROPRO with a range of values assigned to the hydrodynamic radius of the C α pseudoatom; the translational diffusion coefficients computed by HYDROPRO using these pseudoatomic models were then compared with those computed with the *fully atomic* models, and the hydrodynamic radius producing the best overall agreement was selected (note therefore that we use the same hydrodynamic radius for all residue types): the best agreement was obtained with a hydrodynamic radius of 5.3 Å (see above). Repeating the entire procedure for the SC model, an optimal hydro-

dynamic radius was found to be 3.5 Å (see the Supporting Information for further details).

Calculation of Diffusion Coefficients from BD Simulations. For all proteins studied, translational diffusion coefficients were calculated as an average from 10 independent BD simulations, each conducted for a production length of 100 ns following a brief (100 ps) equilibration period. From each trajectory the translational diffusion coefficient, D_{trans} , was computed using the Einstein formula⁴³

$$D_{\text{trans}} = \langle R^2 \rangle / 6\delta t \quad (8)$$

where $\langle R^2 \rangle$ is the mean-squared distance traveled by the protein’s center of geometry in a time interval δt . All of the computed values reported in Results were obtained with $\delta t = 100$ ps, but the results were insensitive to the exact choice of δt (see the Supporting Information).

Rotational diffusion coefficients for folded proteins were also calculated as averages from 10 independent simulations, but longer simulations were required in order to obtain robust estimates: the production length of all such simulations was 500 ns. Rotational motion was quantified by computing time-autocorrelation functions for vectors pointing along the principal axes of the proteins’ moments of inertia; these three axes were approximated by vectors connecting the two pseudoatoms closest to the principal axes of the native state structure. The three autocorrelation functions were averaged, and the first 20 ns of the averaged function were fit to a single exponential (additional exponentials were found to be unnecessary); the time constant for this decay gives the rotational relaxation time τ_{rot} , from which the rotational diffusion coefficient D_{rot} can be calculated as $D_{\text{rot}} = 1/(2\tau_{\text{rot}})$.⁹⁰

In addition to calculating conventional translational and rotational diffusion coefficients for entire proteins, an ‘effective’ diffusion coefficient was also defined as a way of quantifying the *relative* diffusion of pseudoatom pairs as a function of their sequence-separation (see Results). This was achieved by analyzing ten 100 ns BD trajectories of a 108-residue peptide chain simulated (at a C α level of detail) with only non-native nonbonded interactions and with all dihedral angle potentials set to zero. The effective diffusion coefficient, D_{eff} , for the relative motion of two pseudoatoms was determined by applying the one-dimensional Einstein formula to the mean-squared change in the separation *distance* of the two pseudoatoms over the time-interval, $\delta t = 100$ ps. Effective diffusion coefficients defined in this way were computed separately for pseudoatom pairs separated by 2, 4, 6, 8 residues etc. with the two pseudoatoms of each pair being symmetrically located either side of the center of the peptide chain. These calculations were carried out for simulations performed both with and without hydrodynamic interactions.

Folding Simulations. In order to assess the potential impact of HI on the folding kinetics of the proteins, 100 independent folding simulations were performed for all 11 proteins at a C α level of detail and for three proteins (protein L, CSPB, and λ -repressor) at the SC level of detail; each folding simulation started from a different initial conformation generated by randomly assigning dihedral angles such

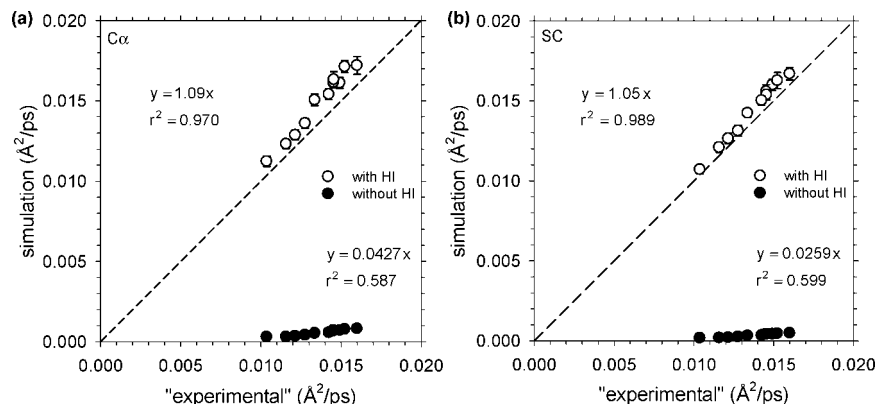


Figure 1. Simulation-derived translational diffusion coefficients of folded proteins plotted against the corresponding ‘experimental’ values (see Methods for the derivation of these experimental values): (a) $C\alpha$ model proteins and (b) side chain (SC) model proteins.

that no steric interactions were included. The extent of folding during the simulations was quantified during the simulations with the conventional structural parameter ‘ Q ’,^{8,39} defined as the number of native contacts present in the current conformation divided by the number of such contacts formed in the fully folded protein. Again, following the approach outlined by Clementi and others, a native contact was considered to have formed when the two pseudoatoms of the contact pair came within a distance $1.2\sigma_{ij}$ where σ_{ij} is their separation distance in the native state structure. Proteins were considered folded when Q reached 0.90 as this approximately reflected the mean Q obtained in simulations of the folded state. Following Koga and Takada,³⁹ rates of folding were calculated as the inverse of the mean folding time.

In addition to following the folding of the protein, the rate at which the initially unfolded protein adopted a collapsed conformation was computed by monitoring the change in the radius of gyration (R_g) versus time. The time required for R_g to drop below 115% of its native state value was considered its ‘collapse’ time; the remainder of the time required to fold (i.e., to reach $Q = 0.90$) was considered the protein’s ‘search’ time. Rates for these two events were calculated in the same manner as the overall folding rate. Finally, to assess any potential connection between folding rates, hydrodynamic interactions, and the relative preponderance of local and nonlocal contacts in the proteins, absolute ‘contact order’ values^{68,91} for all eleven proteins were obtained, either directly from the literature⁶⁸ or as described therein using the program found at the Baker group’s Web site (<http://depts.washington.edu/bakerpg/>).

Simplified Descriptions of Folding Pathways. A simplified description of the folding pathways exhibited by the proteins was obtained by monitoring the order of formation of key structural elements, with the latter being defined here not only as the conventional helices and sheets (identified using DSSP⁹²) but also as *pairs* of contacting elements of secondary structure (i.e., helix-helix, helix-strand, and strand-strand contacts). The folding statuses of those elements possessing at least five inter-residue contacts were monitored during the simulations using a local folding coordinate, Q_{element} , defined for each element, and analogous with the overall ‘ Q ’ value defined for the entire protein (see above).

A structural element was considered folded when its Q_{element} reached 0.80, at which time its rank order in the folding pathway for that particular simulated trajectory was assigned. The mean rank order assigned to each structural element was calculated from the 100 folding trajectories and used to produce a simple vector (containing M dimensions, where M is the number of structural elements monitored during the simulations) that provides a shorthand description of the protein’s folding pathway. The similarity between the folding pathways obtained from simulations performed with and without HI was then determined from the correlation coefficient of the two folding pathway vectors.

Results

Translational and Rotational Diffusion Coefficients.

The computed translational diffusion coefficients of folded proteins obtained from BD simulations, both with and without the inclusion of hydrodynamic interactions (HI), are plotted against the corresponding ‘experimental’ estimates (see Methods) in Figure 1; in (a) are shown the results obtained with a model that treats proteins at a $C\alpha$ level of representation; in (b) are shown the results obtained with a model that includes additional pseudoatoms to account for side chains (SC). With both models it can be seen that the BD simulations that include HI (open circles) reproduce the ‘experimental’ values very well, while the simulations that omit HI (filled circles) produce values that drastically underestimate the expected values. In fact, with the $C\alpha$ model, the translational diffusion coefficients are underestimated on average by a factor of ~ 23 , whereas with the more detailed SC model, they are underestimated by a factor of ~ 39 . Also displayed in Figure 1 (and subsequent figures) are the r^2 values obtained from linear regressions in which an intercept of zero was enforced. Since the translational diffusion coefficients scale inversely with the overall sizes of the proteins, the much poorer quality regression fits obtained from the non-HI simulations indicates that, in addition to underestimating the absolute values of the diffusion coefficients, they also are significantly less able to capture the size-dependence of translational diffusion than are the simulations that include HI.

The above results refer to BD simulations of the proteins performed with parameters in which the native state struc-

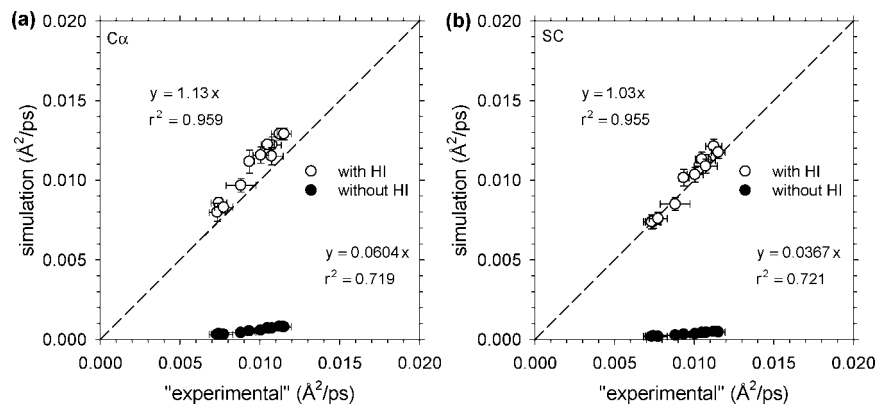


Figure 2. Simulation-derived translational diffusion coefficients of unfolded proteins plotted against the corresponding 'experimental' values: (a) C α model proteins and (b) SC model proteins.

tures are energetically favored. A qualitatively identical picture emerges however when we conduct similar comparisons using BD simulations in which the proteins adopt only unfolded conformations (see Methods): the HI simulations again produce translational diffusion coefficient estimates that match closely with the expected values, while the non-HI simulations again dramatically underestimate them (Figure 2). Interestingly however, the magnitude of the underestimation with non-HI simulations is less than that obtained from folded state simulations: the C α and SC models now underestimate the 'experimental' values by factors of ~ 17 and ~ 27 , respectively. In addition, the quality of the regression fits for the non-HI simulation data are noticeably improved over those shown in Figure 1. It appears therefore that the omission of HI from simulations of unfolded conformations, while still being catastrophic for the simulations' ability to produce quantitatively accurate diffusion coefficients, at least does not completely destroy their ability to capture the diffusion coefficient's dependence on protein size.

The results shown up to this point have shown that the inclusion of HI in BD simulations of model proteins leads to much better descriptions of their translational diffusional behavior, regardless of whether such proteins are simulated in their folded or unfolded states. This conclusion is amplified when we consider the *ratio* of the translational diffusion coefficients for the folded and unfolded states of the proteins. Experimentally it is well-known that the folding of proteins into their globular conformations leads to significant increases in their translational diffusion coefficients.^{93–98} This can be seen from Table 2 where we collate results from six published experimental studies in which the folded and unfolded state diffusion coefficients have been simultaneously reported for proteins of similar sizes to those studied here: the ratios of the folded to unfolded state diffusion coefficients from these studies range from 1.36 to 1.75. This behavior is conspicuously not reproduced by the BD simulations in which HI are neglected: the computed ratio for non-HI simulations is $1.00 (\pm 0.01)$ for both the C α and SC models. The HI simulations on the other hand capture the experimental trend quite well: for the C α and SC models, respective ratios of 1.38 ± 0.08 and 1.47 ± 0.11 are obtained, indicating that the accelerated diffusion that results from

Table 2. Ratios of Translational Diffusion Coefficients of Folded and Unfolded States Computed from Simulation and Measured Experimentally

protein	C α w/HI	C α w/o HI	SC w/HI	SC w/o HI	expt
protein G	1.33	1.01	1.38	1.01	
protein L	1.32	1.02	1.42	0.99	
CI2	1.32	1.01	1.38	1.00	
barnase	1.41	1.00	1.55	1.00	
fyn-SH3	1.33	1.00	1.39	1.00	
CSPB	1.42	1.01	1.41	1.00	
IFABP	1.50	0.99	1.71	1.01	
SFVP	1.54	1.01	1.64	1.01	
λ -repressor	1.33	1.00	1.45	1.01	
Im9	1.35	1.01	1.40	1.00	
apo-CaM	1.36	0.99	1.41	1.01	
BPTI ^a					1.36
CTL9 ^b					1.72
RNase A ^c					1.65
lysozyme ^d					1.69
spc-SH3 ^e					1.32
IFABP ^f					1.75

^a Reference 94. Reduced disulfide bonds in unfolded state.

^b Reference 98. ^c Reference 93. Reduced disulfide bonds in unfolded state. ^d Reference 95. Reduced disulfide bonds in unfolded state. ^e Reference 97. ^f Reference 96. With Alexa bound at V60.

folding can be successfully modeled by implicit-solvent simulations as long as HI are included.

Very similar trends are observed when the rotational diffusion coefficients of the proteins are examined. Figure 3 compares the computed rotational diffusion coefficients of the folded states of the proteins calculated from simulations, both with and without HI, with the corresponding 'experimental' estimates. Again, the values computed from the simulations with HI match very closely with the experimental estimates while those computed from simulations without HI significantly underestimate them; and again, the quality of the linear regression fits are higher for the simulations that include HI, indicating that they more faithfully reproduce the protein size-dependence of the diffusion coefficients. Interestingly however, the magnitude of the error in the non-HI simulations' rotational diffusion coefficients is significantly lower than the error obtained with the translational diffusion coefficients (e.g., compare the slopes of Figure 1a and Figure 3a). This difference suggests that the non-HI simulations are also likely to produce significant errors in the *relative* magnitudes of the translational and rotational

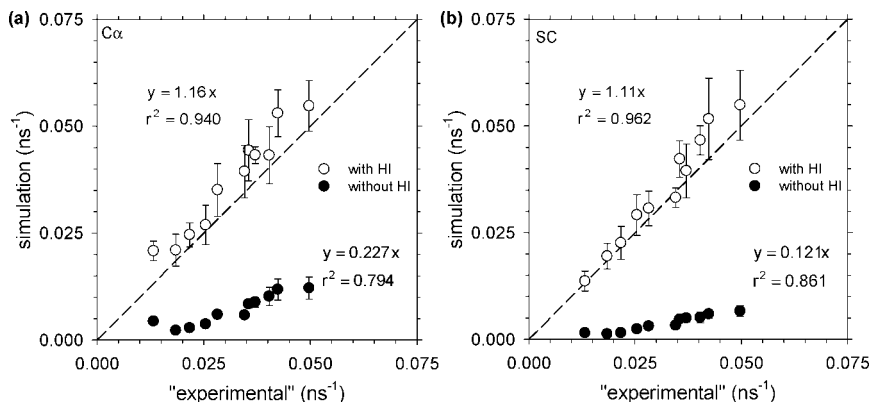


Figure 3. Simulation-derived rotational diffusion coefficients of folded proteins plotted against the corresponding 'experimental' values: (a) C α model proteins and (b) SC model proteins.

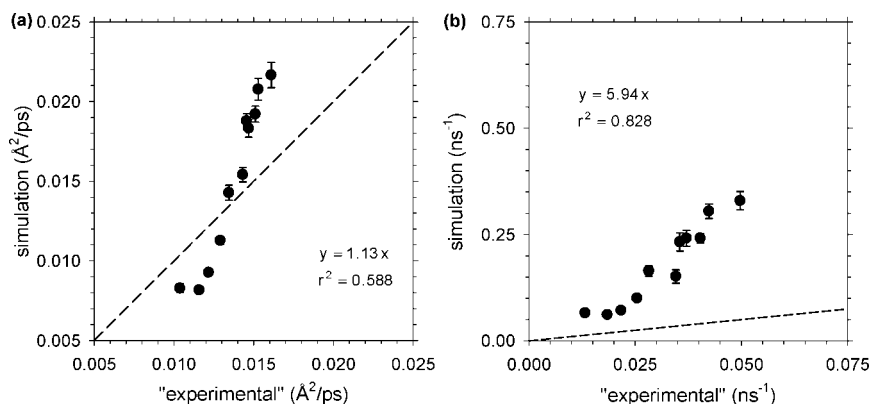


Figure 4. Simulation-derived translational and rotational diffusion coefficients of folded proteins plotted against the corresponding 'experimental' values. All simulations used a C α model, with a hydrodynamic radius of 0.2 Å assigned to all pseudoatoms and neglected hydrodynamic interactions between pseudoatoms: (a) translational diffusion coefficients and (b) rotational diffusion coefficients.

diffusion coefficients, i.e. in the ratio of these two diffusion coefficients. This indeed appears to be the case: the average translational-to-rotational diffusion coefficient ratio for the 11 proteins obtained from the HYDROPRO calculations is $0.47 \pm 0.14 \times 10^3 \text{ Å}^2$, and while the corresponding ratios obtained with HI for the C α and SC models are 0.43 ± 0.09 and $0.46 \pm 0.15 \times 10^3 \text{ Å}^2$, respectively, the ratios obtained without HI for the two models are 0.09 ± 0.03 and $0.11 \pm 0.03 \times 10^3 \text{ Å}^2$, respectively.

The results reported up to this point provide a strong indication that simulations that include HI are much better able to capture all of the investigated aspects of proteins' diffusional behavior than are simulations that neglect HI. As noted in the Discussion, a significant drawback with the HI calculations is their very considerable computational expense; it is therefore worth considering whether simulations that neglect HI (and which have the advantage that they are much faster to compute) could be optimized in some way to better reproduce the experimental behavior. The significant underestimation of both translational and rotational diffusion coefficients suggests that better results might be obtained if an artificially reduced hydrodynamic radius was assigned to the pseudoatoms in non-HI simulations. In fact, a series of simulations using the C α model of the proteins show that a hydrodynamic radius of 0.2 Å can give a reasonably good reproduction of the translational diffusion coefficients (Figure

4a) in the sense that the slope of the linear regression of simulation-derived diffusion coefficients with experimental estimates is now much closer to 1 than is obtained with a more 'reasonable' hydrodynamic radius. Unfortunately, two observations significantly undercut this otherwise promising result. First, the protein size-dependence of the translational diffusion coefficients is poorly reproduced: the translational diffusion coefficients of the smaller proteins (top right of Figure 4a) are consistently overestimated (by up to 35%), while those of the larger proteins (bottom left of the figure) are consistently underestimated (by as much as 30%). Second, the rotational diffusion coefficients of the proteins obtained from the same simulations are overestimated by a factor of ~ 6 (see Figure 4b). These results therefore suggest that a simultaneous reproduction of all of the diffusional properties of a protein in an implicit-solvent model that does not include any modeling of HI will not be possible, even if the hydrodynamic radius of the pseudoatoms is treated as an adjustable parameter.

Folding Simulations. A potential consequence of the diffusional studies presented thus far is that the simulated rates of folding of the same model proteins might also be significantly affected by the inclusion of HI. To address this issue folding rates have been computed for the proteins (both with and without HI) by measuring the time taken to adopt

Table 3. Ratios of the Folding Rates Obtained with HI Included to the Folding Rates Obtained without HI Included^a

protein	C α	SC
α -helix	0.28 \pm 0.04	
β -hairpin	0.73 \pm 0.05	
protein G	1.84 \pm 0.25	
protein L	1.72 \pm 0.40	3.15 \pm 0.18
CI2	1.36 \pm 0.38	
barnase	2.13 \pm 0.28	
fyn-SH3	1.24 \pm 0.17	
CSPB	1.52 \pm 0.27	2.38 \pm 0.60
IFABP	2.29 \pm 0.39	
SFVP	1.86 \pm 0.31	
λ -repressor	1.65 \pm 0.25	3.66 \pm 0.32
Im9	1.69 \pm 0.11	
apo-CaM	1.70 \pm 0.27	

^a Folding rates are computed from the reciprocal of the mean folding time of 100 independent folding trajectories for each protein.

the native conformation in series of 100 independent simulations that start from randomly constructed unfolded conformations; this procedure has been carried out for all 11 proteins with the C α representation and three of the proteins with the SC representation (owing to the significant computational expense of the latter simulations). For comparison purposes, similar simulations have also been run for the folding of a 16-residue α -helix and a 16-residue β -hairpin. The results of all these studies are compiled in Table 3 in the form of ratios of the folding rate computed with HI to the rate computed without HI. For all *proteins* studied, the inclusion of HI causes a significant increase in the computed rate of folding: for the 11 C α models investigated the average ratio is 1.73 ± 0.30 ; for the three SC models studied, the average ratio is 3.07 ± 0.64 , indicating that the acceleration of the folding rate is significantly greater when the more structurally detailed SC model is used.

The effects of HI on the folding rates can be explored in greater detail by examining separately their effect on first, the initial transition from an extended, unfolded conformation to a compact, collapsed conformation, and second, the transition from this collapsed state to the final, native state (see Methods). As might be expected given the large effects of HI on proteins' diffusional characteristics, the primary effect of HI on folding rates is, for the most part, exerted in the initial collapse phase: for the eleven C α model proteins, the ratio of the 'collapse' rates with and without HI is 2.44 ± 0.75 , while the ratio of the 'search' rates with and without HI is 1.34 ± 0.20 (see Table 4). This qualitative picture is preserved for the three SC model proteins that we have studied, although the large error bars for the search ratio of CSPB prevent very firm conclusions being drawn.

The increased folding rates that result from the inclusion of HI when complete proteins are considered is in marked contrast to what is observed when the folding rates of the individual secondary structure elements are measured: for both the α -helix and the β -hairpin the inclusion of HI causes a very significant *decrease* in folding rate (Table 3). In both the α -helix and the β -hairpin the inter-residue contacts that are formed are, by construction, local since both of them are only 16 residues long; in proteins of course, the inter-

Table 4. Ratios of the 'Collapse' and 'Search' Rates Obtained with HI to the Rates Obtained without HI

protein	collapse C α	collapse SC	search C α	search SC
protein G	2.35 \pm 0.38		1.73 \pm 0.29	
protein L	1.96 \pm 0.27	3.38 \pm 0.24	1.30 \pm 0.32	0.86 \pm 0.51
CI2	2.05 \pm 0.21		1.20 \pm 0.35	
barnase	2.79 \pm 0.17		1.47 \pm 0.47	
fyn-SH3	1.37 \pm 0.23		1.13 \pm 0.18	
CSPB	1.89 \pm 0.18	2.35 \pm 0.64	1.19 \pm 0.47	2.41 \pm 3.26
IFABP	2.98 \pm 0.44		1.46 \pm 0.44	
SFVP	2.42 \pm 0.38		1.20 \pm 0.55	
λ -repressor	2.25 \pm 0.78	3.81 \pm 0.34	1.59 \pm 0.11	1.37 \pm 0.63
Im9	2.49 \pm 0.34		1.09 \pm 0.20	
apo-CaM	4.28 \pm 0.70		1.39 \pm 0.27	

residue contacts formed in the native state are of both local and nonlocal origins.⁹¹ One potential explanation for the difference between the two sets of results therefore is that the inclusion of HI accelerates the formation of nonlocal interactions while decelerating the formation of local interactions. This idea has been investigated by analyzing the folding trajectories in more detail: specifically, the time taken for structural elements to fold and associate has been measured and correlated with the number of residues that separate the members of the elements along the polypeptide chain (see Methods). The combined results of such an analysis carried out on all 11 C α model proteins are illustrated by the closed symbols in Figure 5a where the relative rates of association of the pairs of structure elements obtained with and without HI are plotted along the y-axis. Clearly, the plot matches the expectation expressed above: the inclusion of HI decreases somewhat the rate at which closely spaced structure elements come into contact with each other but increases the rate at which more widely spaced structure elements associate.

Since the association rates of structure elements in the model proteins are likely to be influenced by the folding status of intervening structural elements, it is worth considering whether a more direct connection between the association rates of structural elements and the diffusional properties of the polypeptide chain can be obtained. This has been done by performing additional BD simulations of a 108-residue C α -only peptide chain in which no favorable native interactions operate (i.e., one in which the only forces that operate are those acting on pseudobonds and pseudoangles and those acting to prevent steric overlap). From these simulations, an effective translational diffusion coefficient has been defined for each residue pair by applying the one-dimensional Einstein equation (see Methods) to the variation of the inter-residue distance. The ratio of the effective inter-residue diffusion coefficients, D_{eff} , obtained with and without HI is plotted as the open symbols in Figure 5a, from which it can be seen that it matches very well with the ratio of association rates for the structure elements.

The finding that the association and folding of nonlocal structural elements is accelerated more by HI than is the association and folding of more local elements would lead one to expect that the proteins for which nonlocal contacts predominate should exhibit the greatest relative increase in folding rate when HI are included. The average sequence locality of native contacts in proteins can be conveniently

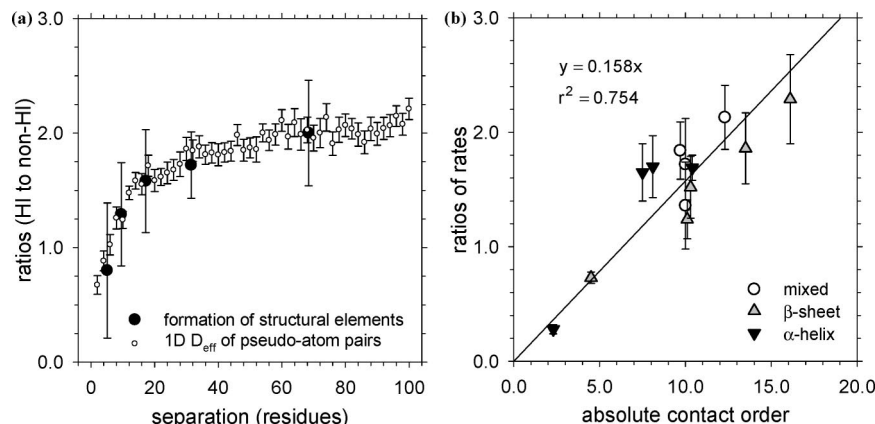


Figure 5. Comparison of the relative rates of folding to relative effective diffusion and absolute contact order. (a) The relative rates of formation of secondary structure elements are compared to the relative D_{eff} of pseudoatoms pairs. From left to right, the first closed symbol represents helices and is offset by one-half the average length of the helices; the remaining closed symbols represent the average separation of pairs of secondary structure elements with separations (as measured by the number of residues between the midpoints of each element) of 6–11, 12–25, 26–39, and 40 and more residues, respectively. (b) The relative rates of folding of the eleven $C\alpha$ model proteins, the α -helix, and the β -hairpin compared to absolute contact order.

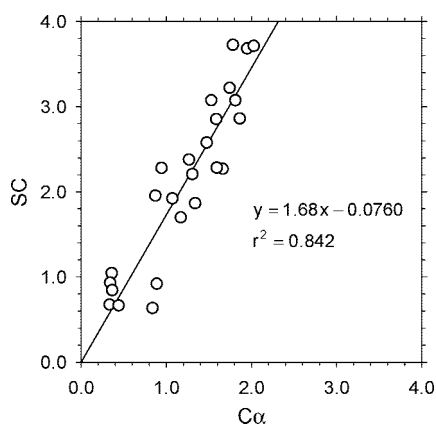


Figure 6. Ratios of the rates of formation of structure elements calculated from simulations using the SC model plotted against those from simulations using the $C\alpha$ model.

represented by the ‘absolute contact order’ measure,⁶⁸ and when plotting the ratio of the folding rates obtained with and without HI against this measure (Figure 5b), we do indeed find that the relative folding rates tend to increase as the prevalence of nonlocal contacts increases. The relationship is especially strong for β -sheet proteins, for which our sample of proteins covers a quite broad range of contact order values, but is unconvincing for the purely α -helical proteins unless the lone α -helix is included in the correlation; this may simply reflect the fact that the range of contact orders of the chosen α -helical proteins is comparatively narrow.

A final issue to note comes from comparing the folding behaviors of the three proteins for which simulations were carried out with both $C\alpha$ and SC models. The same tendency that is observed with $C\alpha$ models for nonlocal interactions to be more accelerated by the inclusion of HI is also seen with the SC models; in fact, a straightforward linear relationship is observed between the HI-induced accelerations of structural element association obtained with the two models (Figure 6). Interestingly, the slope of the linear regression for this plot is 1.68, which matches closely (as

expected) with the ratio of HI-induced accelerations of folding obtained with the two models ($3.07/1.73 = 1.77$).

Finally, we have performed a simple comparison of the folding pathways in the presence and absence of HI by correlating the average rank-order in which the structural elements of each protein formed over 100 folding trajectories (see Methods). Perhaps surprisingly, despite HI’s effect of increasing the relative rates of formation of elements with increasing separation along the peptide chain, the average rank-order in which the elements formed was essentially unaffected: for each of the eleven proteins, the correlation coefficient of the rank-orders obtained with and without HI was at least 0.98 (details shown in the Supporting Information.)

Discussion

Although the modeling of protein folding events has been the subject of a very large number of simulation studies (for reviews, see refs 1–3), very few have considered in detail the diffusional characteristics of the polypeptide chain.^{21,22} The present study has investigated the simulated diffusional properties of 11 proteins and has found that the inclusion of hydrodynamic interactions (HI) between the pseudoatoms of the modeled proteins plays a critical role in allowing these properties to be correctly reproduced. Specifically, the results have indicated that the inclusion of HI dramatically improves the modeling of (a) the translational diffusion coefficient of a flexible protein model, (b) the change in the translational diffusion coefficient that accompanies folding, (c) the rotational diffusion coefficient of a flexible protein model, (d) the relative magnitudes of the translational and rotational diffusion coefficients, and (e) the protein size-dependence of the translational and rotational diffusion coefficients. The fact that all of these properties are correctly captured by simulations that include HI—regardless of the level of structural detail employed in the model—but are very poorly reproduced by simulations that omit HI, argues strongly that some kind of a HI treatment should be included in any molecular simulation that aims to address a problem in which

both diffusion and folding of a protein are likely to be important factors. In passing it is to be noted that while HI arise naturally in simulations that involve explicit solvent, this does not guarantee that a protein's actual diffusional properties will be quantitatively reproduced: in fact, a recent explicit-solvent MD simulation study found the diffusion coefficients of the 76-amino acid protein ubiquitin to be sensitive to both system size (an effect originally identified by Yeh and Hummer⁹⁹) and the water model used.²¹

Before discussing the details and limitations of the particular simulation model used here, it is important to consider the reliability of the 'experimental' estimates for the translational and rotational diffusion coefficients used here. We have chosen to use HYDROPRO^{88,89} as our source of 'gold standard' data here on the basis that for comparing the behavior for a number of different proteins it is important to have reference data that are obtained under identical, standardized conditions. Unfortunately, while there are many experimental estimates available for the translational and rotational diffusion coefficients of proteins, they are only very rarely reported under the same conditions. An attempt to correlate simulated properties with experimental data that are all obtained under slightly different conditions, and/or with different techniques, could be a perilous undertaking, especially given the comparatively small differences in the values for different proteins (e.g., the slowest and fastest diffusing proteins in the current data set have translational diffusion coefficients that differ only by a factor of ~ 1.5). The use of computational estimates from HYDROPRO allows this issue of nonidentical conditions to be avoided, but, of course, it can only be justified if the computational estimates themselves can be considered reliable. Fortunately, from comparisons reported by the group of Garcia de la Torre,^{88,89} it appears that the errors in HYDROPRO's estimates of the translational and rotational diffusion coefficients are very minor (2 and 6%, respectively). Since all of the proteins studied here are similar in size to those examined in the previous comparisons, no special difficulties or errors are likely to arise in the present HYDROPRO estimates.

There are, of course, a number of issues regarding the simulations themselves that must also be addressed. The first is the energy model used to describe inter-residue interactions in the simulations. The 'native-centric' Gō model³⁷ is unashamedly simplified: it does not consider potential favorable non-native interactions and, at least in most implementations, makes no attempt to use different kinds of energy functions to model different kinds of native interactions (e.g., hydrophobic contacts versus salt bridges). Despite these obvious limitations, the model appears surprisingly robust in its ability to describe key aspects of protein folding events:^{8,38–42} the folding rates, for example, of a wide range of single domain proteins can be successfully reproduced by a structural and energetic model that is essentially identical to the one used here,⁴⁰ and, perhaps surprisingly, the same kind of model also appears able to capture changes in stability that are caused by the truncation of the polypeptide chain.⁴² For the bulk of the work that is reported here—i.e. the exploration of the diffusional properties of simulated proteins—the exact details of the energetic

model used in the simulations are, in any case, almost certainly unimportant; we have for example been careful to ascertain that the simulated diffusional properties are unaffected by the choice of the energy well-depth, ϵ , used in the simulations (see the Supporting Information). In fact, for simulating the diffusional properties of the folded states of proteins it is likely that *any* energetic model that retains the proteins roughly in their native shapes (e.g., a Gaussian network model¹⁰⁰) could be used with similar success.

Of course, for modeling actual folding events the details of the energetic model are likely to be more important; however, the key point to note here is that the same energetic and structural models have been used in the simulations that include HI and those that neglect HI. As a consequence, the inherent limitations of the Gō model are also likely to have minimal impact on the central conclusion that has been reached regarding the effects of HI on folding rates: namely, that the inclusion of HI leads to a 2- to 3-fold acceleration of folding, depending on the level of structural detail employed in the model. Importantly, in the Supporting Information we show that this acceleration is not affected by the simulated stability of the protein: varying the energy well-depth, ϵ , associated with all native contacts anywhere within the range 0.55 to 0.65 kcal/mol causes no significant change in the degree to which HI accelerates folding for protein L. Although those results indicate that changing the stability of all contacts simultaneously does not affect the contribution of HI to the folding rate, it could be interesting in the future to examine whether the inclusion of HI affects the rate of formation of different *kinds* of contacts differently, e.g. to see whether HI accelerates formation of favorable electrostatic contacts more than the rate of formation of hydrophobic contacts: given the residue separation-dependence of the HI effect (Figure 5), one might imagine that it could have a greater impact on interactions that can act over longer distances. To investigate this issue however would require the use of an energetic model that is somewhat more sophisticated than the one employed here; interestingly, just such a combined Gō + electrostatic model has already been used recently to investigate the electrostatically accelerated rates of flexible protein-DNA association events.¹⁰¹

A second issue connected with the technical details of the simulations concerns the specific model used to describe the hydrodynamic interactions acting between pseudoatoms. As described in Methods, the model used is one developed independently (as a modification of the Oseen tensor¹⁰² by Rotne and Prager⁷⁶ and Yamakawa⁷⁷); while not the only hydrodynamic model that is available (see for example the somewhat more sophisticated models implemented in the Stokesian dynamics methods of Brady and co-workers¹⁰³), it has been chosen here owing to the fact that it is both readily implemented and is already comparatively widely used in the simulation of macromolecular conformational dynamics. The RPY model has, for example, been used (a) in BD simulations of a flexible loop that acts as a 'gate' for substrate access in the enzyme triose phosphate isomerase,¹⁰⁴ (b) in recent simulations of nucleosomal dynamics in which histone tails are treated at a subresidue level,¹⁰⁵ (c) in simulations of the shear flow-induced unfolding of N-terminus-tethered

ubiquitin,⁵⁵ and (d) in simulations examining the effects of HI on the folding kinetics of simple secondary structure elements^{22,53} (discussed in detail below). The RPY description of HI therefore, while conceived many years ago, still in some respects represents the current ‘state of the art’; this is largely due to the fact that the significant computational resources needed to routinely handle HI calculations in long simulations (see below) have only recently become available. The fact that the modeling of HI with the RPY model apparently produces such a good description of the diffusional characteristics of flexible proteins argues quite strongly that it should find wider application in similar implicit-solvent simulations.

The computational expense associated with the HI calculations employed here should not however be overlooked. Although we have found that one benefit of including HI is that it can allow larger integration timesteps to be used than in simulations that neglect HI (though due to the need to match internal energies for HI and non-HI simulations, we did not always take advantage of this fact; see Methods), this speed-up is nowhere near sufficient to completely offset the additional computational burden involved in their computation. In fact, for the largest protein studied here (apocalmodulin), the computational time required for a simulation performed with HI was 5.6-fold greater than that required for the corresponding non-HI simulation when a C α model was used and was 40-fold greater when a SC model was used. The preceding numbers, it should be remembered, were obtained from simulations that updated the diffusion tensor only every 1 ps or every ~ 25 steps (see Methods); this is an approach commonly used by others,^{106–108} but to ensure that it is appropriate in the present setting, additional control simulations were performed to show that altering the frequency of updates of the HI tensors caused no change in any of the simulation observables (see the Supporting Information). Even with infrequent updates of the hydrodynamic tensors it is clear that for much larger systems the inclusion of HI with the current approach will result in a huge increase in computer time; the development of very fast HI methods—or at least methods that scale better with system size—will therefore likely remain an important pursuit.^{109–111}

It is due to the computational expense of the simulations that we have not carried out a more detailed study of the effects, if any, of the inclusion of HI on the folding mechanisms of the proteins. Ideally, it would be of interest to identify a transition state ensemble (TSE) for each protein, either by finding conformations with ‘Q’ values corresponding to the free energy maximum on the folding free energy landscape^{8,112,113} or by explicitly testing candidate conformations to ensure that they have a 50% chance of proceeding to the folded state (the ‘P_{fold}’ approach).^{114,115} For the present study, both methods are computationally prohibitive: the former approach requires that we first compute the folding free energy landscape as a function of Q, which, in our previous study required simulations of at least 100 μ s for the small protein, CI2;⁴² the latter approach requires that many independent trajectories be run for each candidate conformation in order to obtain reasonable statistical esti-

mates of folding probabilities. Because of these issues, we have chosen to restrict our attention to comparing the order in which the various structural elements fold and assemble in simulations performed with and without HI. It is perhaps surprising that while the inclusion of HI accelerates folding significantly in our simulations, it does not cause any *obvious* change in the folding mechanism, at least insofar as it is reflected in the order of structural element association. Given that we find that HI exerts a stronger effect on the folding and association of elements that are more distantly separated in sequence space, it is not inconceivable that qualitative changes in folding mechanisms might be found for other proteins, especially perhaps for multidomain proteins in which widely separated domains must assemble.

Although the present study provides a reasonably broad comparison of the effects of including HI on protein diffusion and folding, it should be noted that two studies prior to this one have explored HI effects on the folding rates of simpler model systems. The first, and most directly comparable study, is that of Baumketner and Hiwatari²² who investigated the effects of HI on the rates of folding of an α -helix and a β -hairpin, each 16 residues long, using methods very similar to those employed here. In their study, it was reported that HI, modeled using the RPY equations, caused a 2-fold slowing of the folding rate for the β -hairpin but caused no change in the folding rate of the model α helix. The former result is qualitatively similar to what we observe (Table 3); the latter result however contrasts markedly with the 4-fold deceleration of folding that we observe to be caused by HI. As is often the case when comparing simulation studies, it is not easy to determine unambiguously the reason for the discrepancy; possible sources of the difference would appear to be (a) differences in the studies’ energy functions, for both bonded and nonbonded interactions, and (b) the use of the bond constraint algorithm SHAKE in the HI simulations of Baumketner and Hiwatari.²²

The only other work that we are aware of having explored the effects of HI on the folding of a freely diffusing protein is a study reported by the Yeomans’ group⁵³—which used a HI model quite different from that employed here—and which examined the folding of a model α -helix and a β -hairpin, each 19 residues in length, and the folding kinetics of the protein CI2 (referred to as ‘2CI2’ in their paper): in all three cases they found that HI caused a negligible change in the folding kinetics. Again, the technical differences between the present study and the previous work are significant: in particular, the model used by Kikuchi et al.⁵³ (a) models HI with the stochastic rotation dynamics model,¹¹⁶ (b) assigns no energy parameters to pseudodihedral angles of the modeled polypeptides, and (c) uses the radius of gyration as the reaction coordinate for monitoring folding, rather than any more detailed measure of the formation of native contacts. Interestingly, in the same study, Kikuchi et al.⁵³ did find that the rate of *polymer* collapse was accelerated with the inclusion of HI, which is, of course (along with other polymer studies of the coil to globule transition^{50–52}), in agreement with the results presented here.

The fact that so many aspects of the diffusional behavior of the 11 proteins are correctly captured by the present

simulation model gives us confidence that the basic conclusions of the folding studies are also correct. The key results that we have obtained—that folding is accelerated by 2–3-fold due to the inclusion of HI and that this results primarily from the accelerated formation of long-range native contacts—are likely to be of significance in a number of areas. First, the results may have implications for models of protein folding that emphasize the diffusional-search aspects of the process, such as the diffusion-collision model proposed by Karplus and Weaver¹¹⁷ and successfully applied to experimental folding kinetics data by Oas and co-workers.^{118,119} Second, the findings may be significant for very fast-folding (or ‘downhill’ folding¹²⁰) proteins, as suggested by a recent dynamic Monte Carlo simulation where the kinetic transition state barrier was both shifted and increased as a result of configuration-dependent diffusion.¹²¹ Third, they are also likely to be of importance for models and studies that attempt to understand the diffusion-limited kinetics of loop-closure events, an area that has already seen fruitful interplay between experiment and simulation.^{122,123} Fourth, they may be important to keep in mind when attempts are made to directly compare folding kinetics obtained from implicit- and explicit-solvent simulations;¹²⁴ although such comparisons are in any case likely to be severely hampered by differences in the underlying folding free energy landscapes,^{125–128} the present study emphasizes the fact that simulations that use a non-HI implicit solvent model also differ—in a hydrodynamic, rather than an energetic sense—from corresponding explicit-solvent simulations. Finally, it may turn out to be quite important to note that—despite the accelerated folding—proteins modeled with HI diffuse 3–4 times farther during the time it takes them to fold than do proteins modeled without HI (see the Supporting Information). Although this might not be a particularly important observation for modeling of a fundamentally intramolecular event such as single-domain protein folding (after all, we see here no obvious changes in the apparent folding mechanisms caused by HI inclusion), it would seem to have rather obvious implications for modeling the kinetics of intermolecular events such as the coupled folding and binding of proteins¹⁰¹ or peptide- and protein-aggregation processes.¹²⁹ For correct modeling of such situations therefore, the continued development of fast methods for modeling hydrodynamic interactions might prove to be rather important.

Acknowledgment. T.F.K. is grateful for the support of an Iowa Presidential Fellowship. This work was supported in part by a grant to A.H.E. from the Carver Trust.

Supporting Information Available: Details regarding the conversion of all-atom protein structures to reduced pseudoatom models; control simulations for the effect of time-step choice on calculated diffusion coefficients; selection of timesteps for folding simulations and the timestep dependence of the proteins’ simulated energies; the effects of a bond constraint algorithm in simulations with HI; control simulations for the effect(s) of diffusion tensor update interval on simulation observables; finding the optimal hydrodynamic radius for the C α and SC models; control simulations for the effect(s) of observation interval on calculated diffusion coefficients; com-

parison of the folding pathways; control simulations for the effect of standardized energy parameters on calculated diffusion coefficients and the acceleration of folding in simulations with HI; and comparison of the average net distance traveled by the proteins prior to folding. This material is available free of charge via the Internet at <http://pubs.acs.org>.

References

- (1) Daggett, V.; Fersht, A. R. *Nat. Rev. Mol. Cell Biol.* **2003**, *4*, 497–502.
- (2) Onuchic, J. N.; Wolynes, P. G. *Curr. Opin. Struct. Biol.* **2004**, *14*, 70–75.
- (3) Chen, Y.; Ding, F.; Nie, H.; Serohijos, A. W.; Sharma, S.; Wilcox, K. C.; Yin, S.; Dokhoyan, N. V. *Arch. Biochem. Biophys.* **2008**, *469*, 4–19.
- (4) Carrell, R. W.; Lomas, D. A. *Lancet* **1997**, *350*, 134–138.
- (5) Chiti, F.; Dobson, C. M. *Annu. Rev. Biochem.* **2006**, *75*, 333–366.
- (6) Levitt, M.; Warshel, A. *Nature* **1975**, *253*, 694–698.
- (7) Kolinski, A.; Skolnick, J. *Proteins: Struct., Funct., Genet.* **1994**, *18*, 353–366.
- (8) Clementi, C.; Nymeyer, H.; Onuchic, J. N. *J. Mol. Biol.* **2000**, *298*, 937–953.
- (9) Northrup, S. H.; Erickson, H. P. *Proc. Natl. Acad. Sci. U.S.A.* **1992**, *89*, 3338–3342.
- (10) Gabdoulline, R. R.; Wade, R. C. *J. Mol. Biol.* **2001**, *306*, 1139–1155.
- (11) Hagan, M. F.; Chandler, D. *Biophys. J.* **2006**, *91*, 42–54.
- (12) McGuffee, S. R.; Elcock, A. H. *J. Am. Chem. Soc.* **2006**, *128*, 12098–12110.
- (13) Chong, L. T.; Snow, C. D.; Rhee, Y. M.; Pande, V. S. *J. Mol. Biol.* **2005**, *345*, 869–878.
- (14) Periole, X.; Huber, T.; Marrink, S. J.; Sakmar, T. P. *J. Am. Chem. Soc.* **2007**, *129*, 10126–10132.
- (15) Ding, F.; Dokhoyan, N. V.; Buldyrev, S. V.; Stanley, H. E.; Shakhnovich, E. I. *J. Mol. Biol.* **2002**, *324*, 851–857.
- (16) Yang, S. C.; Cho, S. S.; Levy, Y.; Cheung, M. S.; Levine, H.; Wolynes, P. G.; Onuchic, J. N. *Proc. Natl. Acad. Sci. U.S.A.* **2004**, *101*, 13786–13791.
- (17) Smith, A. V.; Hall, C. K. *J. Mol. Biol.* **2001**, *312*, 187–2002.
- (18) Dima, R. I.; Thirumalai, D. *Protein Sci.* **2002**, *11*, 1036–1049.
- (19) Gsponer, J.; Haberthur, U.; Caflisch, A. *Proc. Natl. Acad. Sci. U.S.A.* **2003**, *100*, 5154–5159.
- (20) Matysiak, S.; Clementi, C. *J. Mol. Biol.* **2006**, *363*, 297–308.
- (21) Takemura, K.; Kitao, A. *J. Phys. Chem. B* **2007**, *111*, 11870–11872.
- (22) Baumketner, A.; Hiwatari, Y. *J. Phys. Soc. Jpn.* **2002**, *71*, 3069–3079.
- (23) Taddei, N.; Capanni, C.; Chiti, F.; Stefani, M.; Dobson, C. M.; Ramponi, G. *J. Biol. Chem.* **2001**, *276*, 37149–37154.
- (24) Chiti, F.; Taddei, N.; Baroni, F.; Capanni, C.; Stefani, M.; Ramponi, G.; Dobson, C. M. *Nat. Struct. Biol.* **2002**, *9*, 137–143.

- (25) Rhee, Y. M.; Sorin, E. J.; Jayachandran, G.; Lindahl, E.; Pande, V. S. *Proc. Natl. Acad. Sci. U.S.A.* **2004**, *101*, 6456–6461.
- (26) Jayachandran, G.; Vishal, V.; Pande, V. S. *J. Chem. Phys.* **2006**, *124*, 164902.
- (27) Duan, Y.; Kollman, P. A. *Science* **1998**, *282*, 740–744.
- (28) García, A. E.; Onuchic, J. N. *Proc. Natl. Acad. Sci. U.S.A.* **2003**, *100*, 13898–13903.
- (29) Pitera, J. W.; Swope, W. C.; Abraham, F. F. *Biophys. J.* **2008**, *98*, 4837–4846.
- (30) Zagrovic, B.; Snow, C. D.; Shirts, M. R.; Pande, V. S. *J. Mol. Biol.* **2002**, *323*, 927–937.
- (31) Jagielska, A.; Scheraga, H. A. *J. Comput. Chem.* **2007**, *28*, 1068–1082.
- (32) Still, W. C.; Tempczyk, A.; Hawley, R. C.; Hendrickson, T. *J. Am. Chem. Soc.* **1990**, *112*, 6127–6129.
- (33) Luo, R.; David, L.; Gilson, M. K. *J. Comput. Chem.* **2002**, *23*, 1244–1253.
- (34) Eisenberg, D.; McLachlan, A. D. *Nature* **1986**, *319*, 199–203.
- (35) Ooi, T.; Oobatake, M.; Némethy, G.; Scheraga, H. A. *Proc. Natl. Acad. Sci. U.S.A.* **1987**, *84*, 3086–3090.
- (36) Lazaridis, T.; Karplus, M. *Proteins: Struct., Funct., Genet.* **1999**, *35*, 133–152.
- (37) Taketomi, H.; Ueda, Y.; Gō, N. *Int. J. Pept. Protein Res.* **1975**, *7*, 445–459.
- (38) Hoang, T. X.; Cieplak, M. *J. Chem. Phys.* **2004**, *113*, 8319–8328.
- (39) Koga, N.; Takada, S. *J. Mol. Biol.* **2001**, *313*, 171–180.
- (40) Chavez, L. L.; Onuchic, J. N.; Clementi, C. *J. Am. Chem. Soc.* **2004**, *126*, 8426–8432.
- (41) Das, P.; Wilson, C. J.; Fossait, G.; Wittung-Stafshede, P.; Matthews, K. S.; Clementi, C. *Proc. Natl. Acad. Sci. U.S.A.* **2005**, *102*, 14569–14574.
- (42) Elcock, A. H. *PLoS Comput. Biol.* **2006**, *2*, 824–841.
- (43) Allen, M. P.; Tildesley, D. J. *Computer Simulation of Liquids*; Oxford University Press Inc.: New York, 1989.
- (44) Larson, R. G. *Constitutive equations for polymer melts and solutions*; Butterworths: Boston, 1988.
- (45) Ermak, D. L.; McCammon, J. A. *J. Chem. Phys.* **1978**, *69*, 1352–1360.
- (46) Zimm, B. H. *J. Chem. Phys.* **1956**, *24*, 269–278.
- (47) Kirkwood, J. G.; Riseman, J. *J. Chem. Phys.* **1948**, *16*, 565–573.
- (48) Rouse, P. E. *J. Chem. Phys.* **1953**, *21*, 1272–1280.
- (49) Doi, M.; Edwards, S. F. *International Series of Monographs on Physics 73: The Theory of Polymer Dynamics*; Oxford University Press: New York, 1986.
- (50) Kuznetsov, Y. A.; Timoshenko, E. G.; Dawson, K. A. *J. Chem. Phys.* **1996**, *104*, 3338–3347.
- (51) Pitard, E. *Eur. Phys. J. B* **1999**, *7*, 665–673.
- (52) Kikuchi, N.; Gent, A.; Yeomans, J. M. *Eur. Phys. J. E* **2002**, *9*, 66–66.
- (53) Kikuchi, N.; Ryder, J. F.; Pooley, C. M.; Yeomans, J. M. *Phys. Rev. E* **2005**, *71*, 061804.
- (54) Pham, T. T.; Bajaj, M.; Prakash, J. R. *Soft Matter* **2008**, *4*, 1196–1207.
- (55) Szymczak, P.; Cieplak, M. *J. Chem. Phys.* **2007**, *127*, 155106.
- (56) Gallagher, T.; Alexander, P.; Bryan, P.; Gilliland, G. L. *Biochemistry* **1994**, *33*, 4721–4729.
- (57) O'Neill, J. W.; Kim, D. E.; Baker, D.; Zhang, K. Y. *Acta Crystallogr., Sect. D: Biol. Crystallogr.* **2001**, *57*, 480–487.
- (58) McPhalen, C. A.; James, M. N. *Biochemistry* **1987**, *26*, 261–296.
- (59) Buckle, A. M.; Henrick, K.; Fersht, A. R. *J. Mol. Biol.* **1993**, *234*, 847–860.
- (60) Noble, M. E.; Musacchio, A.; Saraste, M.; Courtneidge, S. A.; Wierenga, R. K. *EMBO J.* **1993**, *12*, 2617–2624.
- (61) Schindelin, H.; Marahiel, M. A.; Heinemann, U. *Nature* **1993**, *364*, 164–168.
- (62) Scapin, G.; Gordon, J. I.; Sacchettini, J. C. *J. Biol. Chem.* **1992**, *267*, 4253–4269.
- (63) Choi, H. K.; Lu, G.; Lee, S.; Wengler, G.; Rossmann, M. G. *Proteins* **1997**, *27*, 345–359.
- (64) Beamer, L. J.; Pabo, C. O. *J. Mol. Biol.* **1992**, *227*, 177–196.
- (65) Osborne, M. J.; Breeze, A. L.; Lian, L. Y.; Reilly, A.; James, R.; Kleanthous, C.; Moore, G. R. *Biochemistry* **1996**, *35*, 9505–9512.
- (66) Kuboniwa, H.; Tjandra, N.; Grzesiek, S.; Ren, H.; Klee, C. B.; Bax, A. *Nat. Struct. Biol.* **1995**, *2*, 768–766.
- (67) Berman, H. M.; Westbrook, J.; Feng, Z.; Gilliland, G.; Bhat, T. N.; Weissig, H.; Shindyalov, I. N.; Bourne, P. E. *Nucleic Acids Res.* **2000**, *28*, 235–242.
- (68) Ivankov, D. N.; Garbuzynskiy, S. O.; Alm, E.; Plaxco, K. W.; Baker, D.; Finkelstein, A. V. *Protein Sci.* **2003**, *12*, 2057–2062.
- (69) Vriend, G. *J. Mol. Graph.* **1990**, *8*, 52–56.
- (70) Wallqvist, A.; Ullner, M. *Proteins: Struct., Funct., Genet.* **1994**, *18*, 267–280.
- (71) Zacharias, M. *Protein Sci.* **2003**, *12*, 1271–1282.
- (72) Ferrenberg, A. M.; Swendsen, R. H. *Phys. Rev. Lett.* **1988**, *61*, 2635–2638.
- (73) Ferrenberg, A. M.; Swendsen, R. H. *Phys. Rev. Lett.* **1989**, *63*, 1195–1198.
- (74) Plaxco, K. W.; Baker, D. *Proc. Natl. Acad. Sci. U.S.A.* **1998**, *95*, 13591–13596.
- (75) Knott, M.; Kaya, H.; Chan, H. S. *Polymer* **2004**, *45*, 623–632.
- (76) Rotne, J.; Prager, S. *J. Chem. Phys.* **1969**, *50*, 4831–4837.
- (77) Yamakawa, H. *J. Chem. Phys.* **1970**, *53*, 436–443.
- (78) Larson, R. G. *Mol. Phys.* **2004**, *102*, 341–351.
- (79) Dalquist, G.; Bjork, A. *Numerical methods*. Prentiss Hall: Englewood Cliffs: NJ, 1974.
- (80) Schlick, T.; Beard, D. A.; Huang, J.; Strahs, D. A.; Qian, X. L. *IEEE Comp. Sci. Eng.* **2000**, *2*, 38–51.
- (81) Hurle, M. R.; Michelotti, G. A.; Crisanti, M. M.; Matthews, C. R. *Proteins* **1987**, *2*, 54–63.

- (82) Jacob, M.; Schindler, T.; Balbach, J.; Schmid, F. X. *Proc. Natl. Acad. Sci. U.S.A.* **1997**, *94*, 5622–5627.
- (83) Ryckaert, J. P.; Ciccotti, G.; Berendsen, H. J. C. *J. Comput. Phys.* **1977**, *23*, 327–341.
- (84) Hess, B.; Bekker, H.; Berendsen, H. J. C.; Fraaije, J. G. E. M. *J. Comput. Chem.* **1997**, *8*, 1463–1472.
- (85) Allison, S. A.; McCammon, J. A. *Biopolymers* **1984**, *23*, 167–187.
- (86) Price, W. S.; Tsuchiya, F.; Arata, Y. *J. Am. Chem. Soc.* **1999**, *121*, 11503–1512.
- (87) Masuda, A.; Ushida, K.; Nishimura, G.; Kinjo, M.; Tamura, M.; Koshino, H.; Yamashita, K.; Kluge, T. *J. Chem. Phys.* **2004**, *121*, 10787–10793.
- (88) Garcide la Torre, J.; Huertas, M. L.; Carrasco, B. *Biophys. J.* **2000**, *78*, 719–730.
- (89) Garcide la Torre, J. *Biophys. Chem.* **2001**, *93*, 159–170.
- (90) Creighton, T. E. *Proteins: Structures and Molecular Properties*; W.H. Freeman & Co. Ltd.: New York, 1992.
- (91) Plaxco, K. W.; Simons, K. T.; Baker, D. *J. Mol. Biol.* **1998**, *277*, 985–994.
- (92) Kabsch, W.; Sander, C. *Biopolymers* **1983**, *22*, 2577–2637.
- (93) Noppert, A.; Gast, K.; Muller-Frohne, M.; Zirwir, D.; Damashun, G. *FEBS Lett.* **1996**, *380*, 179–182.
- (94) Pan, H.; Barany, G.; Woodward, C. *Protein Sci.* **1997**, *6*, 1985–1991.
- (95) Wilkins, D. K.; Grimshaw, S. B.; Receveur, V.; Dobson, C. M.; Jones, J. A.; Smith, L. J. *Biochemistry* **1999**, *38*, 16424–16431.
- (96) Chattopadhyay, K.; Saffarian, S.; Elson, E. L.; Frieden, C. *Biophys. J.* **2005**, *88*, 1413–1422.
- (97) Casares, S.; Sadqi, M.; Lopez-Mayorga, O.; Conejero-Lara, F.; van Nuland, N. A. J. *Biophys. J.* **2004**, *86*, 2403–2413.
- (98) Li, Y.; Shan, B.; Raleigh, D. P. *J. Mol. Biol.* **2007**, *368*, 256–262.
- (99) Yeh, I. C.; Hummer, G. *J. Phys. Chem. B* **2004**, *108*, 15873–14879.
- (100) Haliloglu, T.; Bahar, I.; Erman, B. *Phys. Rev. Lett.* **1997**, *79*, 3090–3093.
- (101) Levy, Y.; Onuchic, J.; Wolynes, P. G. *J. Am. Chem. Soc.* **2007**, *129*, 738–739.
- (102) Oseen, C. W. *Neuere Methoden und Ergebnisse in der Hydrodynamik*; Akademische Verlagsgesellschaft: Leipzig, 1927.
- (103) Brady, J. F.; Bossis, G. *Ann. Rev. Fluid Mech.* **1988**, *20*, 111–157.
- (104) Wade, R. C.; Davis, M. E.; Luty, B. A.; Madura, J. D.; McCammon, J. A. *Biophys. J.* **1993**, *64*, 9–15.
- (105) Arya, G.; Zhang, Q.; Schlick, T. *Biophys. J.* **2006**, *91*, 133–150.
- (106) Jian, H. M.; Schlick, T.; Vologodskii, A. *J. Mol. Biol.* **1998**, *284*, 287–296.
- (107) Huang, J.; Schlick, T.; Vologodskii, A. *Proc. Natl. Acad. Sci. U.S.A.* **2001**, *98*, 968–973.
- (108) Klenin, K.; Merlitz, H.; Langowski, J. *Biophys. J.* **1998**, *74*, 780–788.
- (109) Fixman, M. *Macromolecules* **1986**, *19*, 1204–1207.
- (110) Sierou, A.; Brady, J. F. *J. Fluid Mech.* **2001**, *448*, 115–146.
- (111) Geyer, T.; Winter, U. *Soft Cond. Matt.* [Online] 2008, arXiv: 0801.3212v1.
- (112) Onuchic, J. N.; Socci, N. D.; LutheySchulten, Z.; Wolynes, P. G. *Fold. Des.* **1996**, *1*, 441–450.
- (113) Nymeyer, H.; Socci, N. D.; Onuchic, J. N. *Proc. Natl. Acad. Sci. U.S.A.* **2000**, *97*, 634–639.
- (114) Du, R.; Pande, V. S.; Grosberg, A. Y.; Tanaka, T.; Shakhnovich, E. S. *J. Chem. Phys.* **1998**, *108*, 334–350.
- (115) Li, L.; Shakhnovich, E. I. *Proc. Natl. Acad. Sci. U.S.A.* **2001**, *98*, 13014–13018.
- (116) Malevanets, A.; Kapral, R. *J. Chem. Phys.* **1999**, *110*, 8605–8613.
- (117) Karplus, M.; Weaver, D. L. *Biopolymers* **1979**, *18*, 1421–1437.
- (118) Burton, R. E.; Myers, J. K.; Oas, T. G. *Biochemistry* **1998**, *16*, 5337–5343.
- (119) Myers, J. K.; Oas, T. G. *Nat. Struct. Biol.* **2001**, *8*, 552–558.
- (120) Garcia-Mira, M. M.; Sadqi, M.; Fischer, N.; Sanchez-Ruiz, J. M.; Muñoz, V. *Science* **2002**, *298*, 2191–2195.
- (121) Chahine, J.; Oliveira, R. J.; Leite, V. B. P.; Wang, J. *Proc. Natl. Acad. Sci. U.S.A.* **2007**, *104*, 14646–14651.
- (122) Yeh, I. C.; Hummer, G. *J. Am. Chem. Soc.* **2002**, *124*, 6563–6568.
- (123) Fierz, B.; Kiefhaber, T. *J. Am. Chem. Soc.* **2007**, *129*, 672–679.
- (124) Snow, C. D.; Sorin, E. J.; Rhee, Y. M.; Pande, V. S. *Annu. Rev. Biomol. Struct.* **2005**, *34*, 43–69.
- (125) Zhou, R.; Berne, B. J. *Proc. Natl. Acad. Sci. U.S.A.* **2002**, *99*, 12777–12782.
- (126) Nymeyer, H.; García, A. E. *Proc. Natl. Acad. Sci. U.S.A.* **2003**, *100*, 13934–13939.
- (127) Zhou, R. *Proteins: Struct., Funct., Genet.* **2003**, *53*, 148–161.
- (128) Roe, D. R.; Okur, A.; Wickstrom, L.; Hornak, V.; Simmerling, C. *J. Phys. Chem. B* **2007**, *111*, 1846–1857.
- (129) Nguyen, H. D.; Hall, C. K. *J. Biol. Chem.* **2005**, *280*, 9074–9082.

CT800499P